mode 1 and inclusions or impurities in mode 2. Tomasko *et al.* (*12*) found that mode 1 alone is not sufficient if the particles are sulfur, and that some absorption must reside in mode 2. Inclusions might be solid sulfur or meteoric dust, and impurities in solution might be derived from the latter. It is unlikely that any cloud particle remains pure given lengthy residency with the highly concentrated mode 1 aerosol.

Young (*16*) has generated a convincing fit to the reflection spectrum of Venus by postulating the presence of large particles of solid sulfur at and below an optical depth of 4. Further, a statistical association of dark areas with decreasing CO_2 absorption has been interpreted by Crisp and Young (*17*) as an association with rising cloud tops and therefore upward motion. They have suggested that the updraft carries the (large) particles up to a level where they are more visible. At least at the sounder probe entry location we found no sign of such large particles until we reached such large optical depths that they could have no effect on the reflected radiation. We were at first puzzled by the discrepancy until we realized that small particles are carried up at least as efficiently as large ones. The mechanism can perhaps be rescued if the absorbing particles are smaller than the scattering ones. An essential element of Young's fit to the optical absorption was a specific height (and therefore temperature) distribution of the sulfur particles. It remains to be shown that such a fit can be recaptured with the different distribution that seems to be implied by the Pioneer Venus results.

Mass loading and fluxes. The mass balance is of particular interest in the middle and lower cloud regions. The partitioned mass loading is presented in Fig. 2 with the mass flux for mode 3 in the middle and lower cloud regions. In converting the measured particle-size distributions to profiles of mass loading, we have assumed the particles to be spherical, of density 1.8 g cm^{-3}, and falling at Stokes velocities with zero updraft; a value of 2.5 cm sec^{-1} is computed for the mean mass size. The mode 3 particles in the middle cloud region are most likely nonspherical and could even be needlelike, if sulfur. If so, the mass loading could be overestimated by factors as large as 2.

The peak computed mass flux of 2.8×10^{-3} g m^{-2} sec^{-1}, if representative of the whole planet, must be balanced by a similar upward flux in the gas phase. Values of a few centimeters per second are required; similar values are typically computed from the convergence of the low-level flow associated with terrestrial stratiform clouds.

The mass flux observed also gives rise to a significant heat flux (involving heats of formation as well as latent heats) of 8 W m^{-2}, which equals one-fourth of the solar net flux input at the same altitude range (*3*). Because our computations are so sensitive to size ($\sim r^5$), the values computed must be regarded as estimates (*18*); it is clear, however, that this heat flux may be a thus-far overlooked major component of the overall atmospheric thermal balance, especially when computations indicate the possibility of growth by coalescence to sizes a factor of 2 larger than those actually observed. This comparison is even more significant if it is assumed that our measurements are representative of the whole planet since the planetwide net solar flux would average about 20 percent less than typical measurements by the sounder probe (*3*).

Although the general morphological features of the cloud system are as yet unclear, they appear to be more like stratiform than cumuliform clouds. The potential for mist and drizzle is there, but heavy precipitation is extremely unlikely. Intriguing microphysical questions remain: Can solid elemental sulfur be made to fit all constraints on the mode 3 middle cloud particles? What possible growth mechanisms can force H_2SO_4 droplets to be monodispersed planetwide over great depths? What kind of charge separation processes can operate in clouds of strong electrolyte, and are these clouds really involved in the observed lightning and atmospheric electrification processes? It appears likely that laboratory experimentation will be necessary to provide positive answers to such questions.

ROBERT G. KNOLLENBERG
Particle Measuring Systems, Inc., Boulder, Colorado 80301
D. M. HUNTEN
University of Arizona, Tucson 85724

References and Notes

1. R. G. Knollenberg and D. M. Hunten, *Science*, **203**, 792 (1979).
2. Given sufficient time, populations of identical chemical composition but differing size cannot easily coexist, because size differences imply different vapor equilibrium conditions (Kelvin effect). Ordinarily, the larger particles grow at the expense of the smaller ones, the process becoming more rapid with decreasing size.
3. M. G. Tomasko, L. R. Doose, J. Palmer, A. Holmes, W. Wolfe, N. D. Castillo, P. H. Smith, *Science* **203**, 795 (1979).
4. B. Ragent and J. Blamont, *ibid.*, p. 790.
5. J. B. Pollack *et al.*, *ibid.* **205**, 76 (1979).
6. J. E. Hansen and H. W. Hovenier, *J. Atmos. Sci.* **31**, 1137 (1974).
7. J. Blamont and B. Ragent, *Science* **205**, 67 (1979).
8. M. Ya. Marov, V. N. Lebedev, V. E. Lysteev, I. S. Kuznetsov, G. K. Popandopulo, paper presented at the 19th meeting of the Committee on Space Research of the International Council of Scientific Unions, Philadelphia, 14 to 19 June 1976.
9. *International Critical Tables* (McGraw-Hill, New York, 1926-1930), vol. 7, p. 65.
10. A. T. Young, *Geophys. Res. Lett.*, 49 (1979).
11. M. Ya. Marov, *Annu. Rev. Astron. Astrophys.* **16**, 141 (1978).
12. M. G. Tomasko, L. R. Doose, P. H. Smith, *Science* **205**, 80 (1979).
13. C. E. Junge, *Adv. Geophys.* **4**, 1 (1958).
14. L. D. Travis, D. L. Coffeen, J. E. Hansen, K. Kawabata, A. A. Lacis, W. A. Lane, S. S. Limaye, P. H. Stone, *Science* **203**, 781 (1979).
15. J. Rosinski and R. H. Snow, *J. Meteorol.* **18**, 736 (1961).
16. A. T. Young, *Icarus* **32**, 1 (1977).
17. D. Crisp and A. T. Young, *ibid.* **35**, 183 (1978).
18. While errors in size would be significant at the large sizes contributing the flux, the LCPS also has greater accuracy at these sizes, and a 10 percent error in sizing (largest systematic error estimate) would lead to a factor of only 1.6 flux error.

21 May 1979

Cloud Images from the Pioneer Venus Orbiter

Abstract. *Ultraviolet images of Venus over a 3-month period show marked evolution of the planetary scale features in the cloud patterns. The dark horizontal Y feature recurs quasi-periodically, at intervals of about 4 days, but it has also been absent for periods of several weeks. Bow-shaped features observed in Pioneer Venus images are farther upstream from the subsolar point than those in Mariner 10 images.*

The earliest ultraviolet images of Venus obtained by the cloud photopolarimeter on board the Pioneer Venus orbiter were at moderately large phase angles, thus showing substantially less than the full disk (*1*). The imaging during a nearly 3-month period beginning in early January 1979 has had much more favorable illumination conditions and permits an examination of not only the 4- to 5-day quasi-periodicity but also the long-term variation in the global cloud morphology. We present a representative set of enhanced (*2*) images selected from that period. A list of the seven images, their dates of acquisition, and the time, phase angle, and latitude (*3*) corresponding to the disk center are given in Table 1.

The series of five images shown in Fig. 1 covers a 6-day period and illustrates the recurrence of the dark horizontal Y feature. Although the second image (Fig. 1B) resembles the images from Mariner 10, the rest of this series shows a rapid evolution of the large-scale cloud patterns. Changes in appearance on even

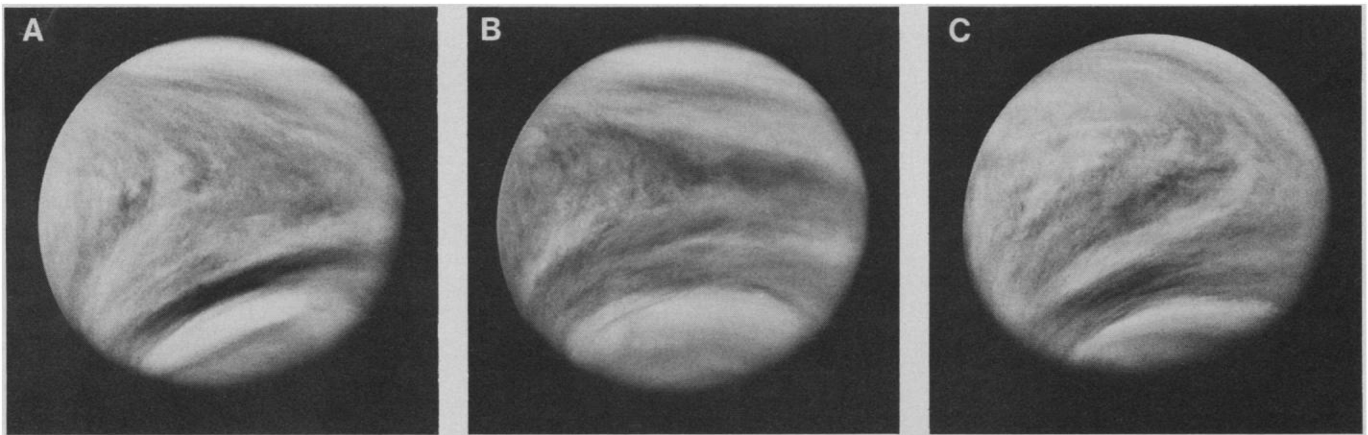

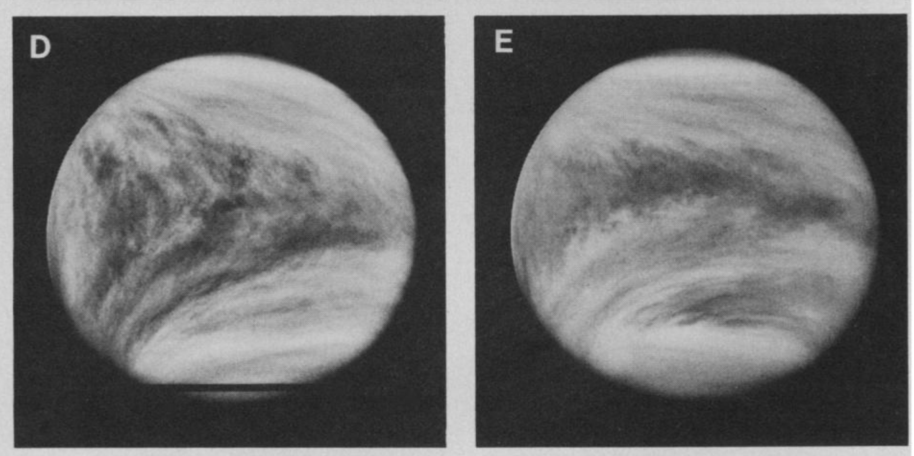

Fig. 1. A sequence of five images illustrating the development and variability of the ultraviolet cloud features over a 6-day period. The first two images, 190 and 194 (A and B), are separated by 1 day and show a feature that with some difficulty may be identified as a dark horizontal Y shape moving into view from the right. The Y appears to be produced by a combination of features, namely (i) a dark equatorial band that is broader in the downstream direction and that joins two dark bands stretching from low to middle latitudes in the downstream direction; (ii) a tilted, bright south polar band and associated bright streaks nearly parallel to the dark bands; and (iii) bow-shaped features often located in the vertex region of the Y. The variation in appearance of each of these features produces the change in the appearance of the Y feature from one recurrence to the next. The relative contrast and shape of the Y in (B) are not symmetric about the equator; such asymmetry is characteristic of the preceding 12 days and similar to that in the Mariner 10 images (5). The next three images—199, 202, and 204 (C to E)—show a very different Y feature moving across the disk. (D) A Y feature that is much more symmetrical and generally broader than the more typical Y 4 days earlier (B). The arms of the Y are formed by several bow-shaped features, which along with the small-scale cellular structure in the center of the disk, give this Y a mottled appearance. The progression in images (C to E) indicates a single Y feature stretching nearly all the way around the planet. Although a similar but shorter Y shape appeared 4 days later, the pattern broke down after that, becoming a more distorted feature as in (B) before disappearing altogether. The region between the bright south polar band and the morning terminator in (A) became considerably brighter as it moved farther onto the disk in (B), illustrating a general tendency for low contrast near the morning terminator. Image (C) shows a number of faint circumequatorial belts identified by Mariner 10 but seen only rarely in the current images. The south polar band in (E) exhibits a "kink" near its left-hand extremity, and the northern edge of the band is disrupted by a series of dark tilted streaks, a condition observed on many occasions.

Table 1. Image acquisition information.

Image number	Date (1979)	Image center: Time (universal time)	Phase angle	Latitude (south)
98	18 Jan.	06:02	51°	22°
190	10 Feb.	09:27	15°	15°
194	11 Feb.	08:44	16°	17°
199	14 Feb.	03:42	27°	29°
202	15 Feb.	08:30	15°	17°
204	16 Feb.	09:08	13°	16°
291	7 Mar.	10:54	34°	9°

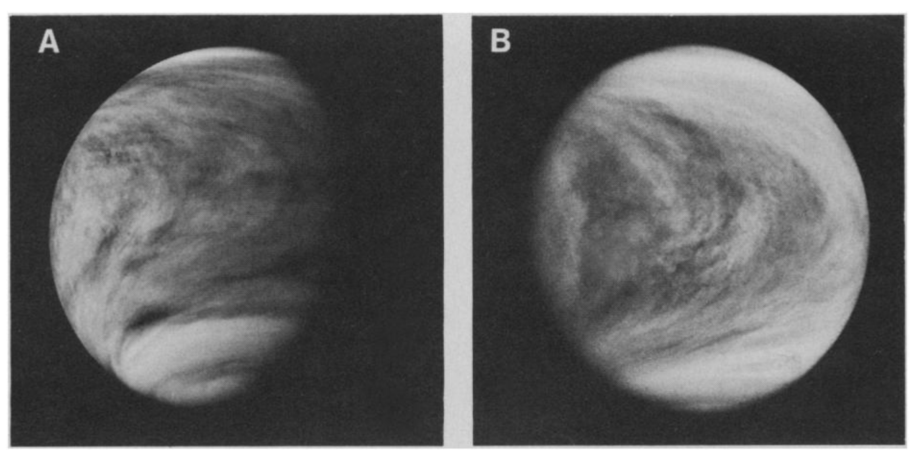

Fig. 2. Images 98 (A) and 291 (B) showing the region near the morning and evening terminators, respectively, during an absence of the large-scale Y feature. These images demonstrate the presence of bow-shaped features as far upstream and downstream of the subsolar point as it is possible to observe. Image (A) resembles the Mariner 10 images except that bow shapes are evident in the morning quadrant and that it is the only image other than 199 (Fig. 1C) among those we have examined to show circumequatorial belts. Image (B) exhibits several bow-shaped features in the afternoon quadrant that form the classical "reverse C" shape observed in low resolution from Earth. When viewed in greater detail, several of the bow shapes appear to be partially composed of "chains" of small polygonal cellular features. Comparisons of these two images illustrate the generally higher contrasts near the evening terminator (B) than near the morning terminator (A), a tendency noted in other such image pairs.

longer time scales can be observed in the 3 months of images now available. For example, there have been two periods, lasting several weeks, during which the Y feature was not apparent even though some of its component parts were present. Bow-shaped features (*4, 5*), which often play an important role in the appearance of the Y feature, have generally been present. The Y feature was absent when the pair of images shown in Fig. 2 were obtained. These images show the morning quadrant approximately 1 month before the series in Fig. 1 and the evening quadrant 1 month after it. The earlier image exhibits bow shapes near the morning terminator, obviously farther upstream from the subsolar point than in Mariner 10 images. The entire 3-month sequence shows small cellular features throughout the low latitudes and occasionally at latitudes as high as ~50°.

The examination and categorization of the ultraviolet cloud features and their evolution is but the first, modest step in attempting to characterize the basic dynamical state of the upper atmosphere and its interaction with the cloud physics. Interpretation of the cloud patterns must be made cautiously because of their diffuse nature (*6*) and the uncertainty regarding the nature of the absorbing and scattering material responsible for the features. At least three different cloud materials contribute to the appearance of the images: (i) an optically thin, high-altitude haze of submicron aerosols (*1*), which is most prevalent near the morning terminator and polar regions; (ii) the diffuse sulfuric acid smog of 1-μm droplets composing the main visible cloud (*7*); and (iii) the ultraviolet absorber located within or below the main visible region of sulfuric acid droplets (*1*). It is possible to define the nature and distribution of these different aerosols more precisely from analysis of polarization measurements obtained by the cloud photopolarimeter. Other key aids are provided by the wind velocities implied by the displacement of small-scale cloud features in successive images and spectral analyses of cloud brightness. These analyses are in progress.

L. D. TRAVIS, D. L. COFFEEN
A. D. DEL GENIO, J. E. HANSEN
K. KAWABATA, A. A. LACIS
W. A. LANE, S. S. LIMAYE
W. B. ROSSOW
NASA Goddard Institute for Space Studies, Goddard Space Flight Center, New York 10025
P. H. STONE
Department of Meteorology, Massachusetts Institute of Technology, Cambridge 02139

References and Notes

1. The initial imaging and polarimetry results were described by L. D. Travis, D. L. Coffeen, J. E. Hansen, K. Kawabata, A. A. Lacis, W. A. Lane, S. S. Limaye, P. H. Stone, *Science* **203**, 781 (1979).
2. Contrast enhancement was performed with high-pass spatial filtering, with scales larger than about 20 percent of the disk diameter excluded. The images presented here are a linear combination of the original data and the high-pass-filtered version, weighted to reveal both the small- and large-scale features.
3. The time given is spacecraft event time in universal time. Phase angle is the angle between the sun-planet and planet-spacecraft directions. The latitudes listed are celestial latitudes, that is, measured from a plane parallel to the ecliptic. The images are oriented with the north pole at the top such that cloud motions from right to left correspond to the retrograde circulation.
4. We use the terminology "bow-shaped features" in the sense of curved or bent, rather than "bowlike waves" (*5*) in the sense of waves generated by the bow of a ship. A term based on morphology rather than on an implicit physical interpretation seems preferable in view of the uncertainty regarding origin of these features.
5. B. C. Murray *et al.*, *Science* **183**, 1307 (1974); M. J. S. Belton, G. R. Smith, D. A. Elliott, K. Klaasen, G. E. Danielson, *J. Atmos. Sci.* **33**, 1383 (1976); M. J. S. Belton, G. R. Smith, G. Schubert, A. D. Del Genio, *ibid.*, p. 1394.
6. K. Kawabata and J. E. Hansen, *J. Atmos. Sci.* **32**, 1133 (1975); A. A. Lacis, *ibid.*, p. 1107.
7. J. E. Hansen and J. W. Hovenier, *ibid.* **31**, 1137 (1974).
8. D.L.C. and W.A.L. were supported by NASA grant 33-015-165 to State University of New York at Stony Brook. A.D.D. and S.S.L. are NASA-NRC resident research associates.

15 May 1979

Nature of the Ultraviolet Absorber in the Venus Clouds: Inferences Based on Pioneer Venus Data

Abstract. *Several photometric measurements of Venus made from the Pioneer Venus orbiter and probes indicate that solar near-ultraviolet radiation is being absorbed throughout much of the main cloud region, but little above the clouds or within the first one or two optical depths. Radiative transfer calculations were carried out to simulate both Pioneer Venus and ground-based data for a number of proposed cloud compositions. This comparison rules out models invoking nitrogen dioxide, meteoritic material, and volatile metals as the source of the ultraviolet absorption. Models involving either small (~ 1 micrometer) or large (~ 10 micrometers) sulfur particles have some serious difficulties, while ones invoking sulfur dioxide gas appear to be promising.*

Beginning at a wavelength of about 0.52 μm, the spherical albedo of Venus steadily declines from a value close to unity to a value of about 0.4 at 0.3 μm (*1*) (Fig. 1). Because clouds totally envelop the surface and are optically thick, this reduction in reflectivity toward the ultraviolet (UV) must be due to some atmospheric component located within or above the main cloud layer. Variations in the properties of the UV-absorbing agent, such as its location with respect to the cloud tops, are believed to be responsible for the marked contrast shown by Venus at wavelengths below about 0.4 μm (*1, 2*).

Strong evidence suggests that concentrated sulfuric acid droplets are the dominant cloud-particle species near the tops of the main cloud deck (*3*), and more limited evidence indicates that it is also present in significant amounts throughout the main cloud layer (*4*). Sulfuric acid is transparent in the blue and near-UV (*5*), however, and so is not the UV-absorbing agent. It has been suggested that the sulfur-containing gases, which serve as precursors for the sulfuric acid particles, might also give rise to elemental sulfur particles and that the sulfur particles are the UV-absorbing agent (*2, 6*). Assuming that the sulfur particles are about 10 μm in size and that they are located only below an optical depth of several, Young (*2*) has obtained a quantitative fit to the wavelength de-

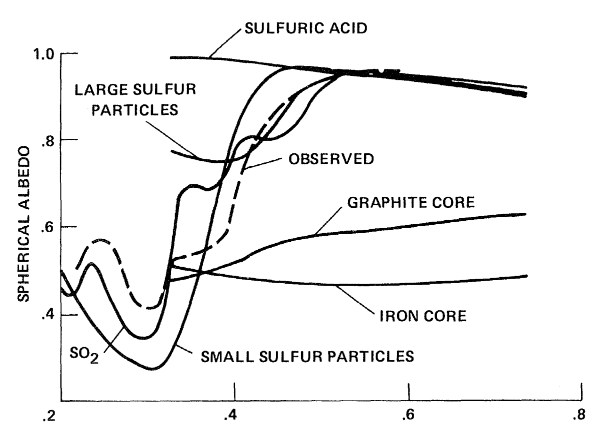

Fig. 1. Comparison of the observed spectral dependence of the spherical albedo of Venus (*1*) and the predicted behavior of several models.